Infection, Genetics and Evolution 68 (2019) 253–264

Contents lists available at ScienceDirect

Infection, Genetics and Evolution

journal homepage: www.elsevier.com/locate/meegid

^{1}H nuclear magnetic resonance-based metabolic profiling of cerebrospinal fluid to identify metabolic features and markers for tuberculosis meningitis

Peixu Zhang[a], Weiguanliu Zhang[a], Yue Lang[a], Yan Qu[b], Jiafeng Chen[a], Li Cui[a,*]

[a] Department of Neurology, First Hospital, Jilin University, Changchun 130021, China
[b] Blood Bank, Jilin Women and Children Health Hospital, Changchun 130021, China

ARTICLE INFO

Keywords:
Tuberculosis meningitis (TBM)
Viral meningitis (VM)
Bacterial meningitis (BM)
Metabolomics
Metabolic profiling
Cerebrospinal fluid (CSF)

ABSTRACT

Background: Tuberculosis meningitis (TBM) is the most severe form of tuberculosis, and currently lacks efficient diagnostic approaches. Metabolomics has the potential to differentiate patients with TBM from those with other forms of meningitis and meningitis-negative individuals. However, no systemic metabolomics research has compared the cerebrospinal fluid (CSF) of these patients.

Methods: ^{1}H nuclear magnetic resonance (NMR) was used for CSF metabolic profiling. Principal component analysis and orthogonal signal correction-partial least squares-discriminant analysis (OPLS-DA) were used to screen for important variables. The Human Metabolome Database was used to identify metabolites, and MetaboAnalyst 4.0 was used for pathway analysis and over-representation analysis.

Results: OPLS-DA modeling could distinguish TBM from other forms of meningitis, and several significantly changed metabolites were identified. Additionally, 23, 6, and 21 metabolites were able to differentiate TBM from viral meningitis, bacterial meningitis, and meningitis-negative groups, respectively. Pathway analysis indicated that these metabolites were mainly involved in carbohydrate and amino acid metabolism, and over-representation analysis indicated that some of these pathways were over-represented.

Conclusions: The metabolites identified have the potential to serve as biomarkers for TBM diagnosis, and carbohydrate and amino acid metabolism are perturbed in the CSF of patents with TBM. Metabolomics is a valuable approach for screening TBM biomarkers. With further investigation, the metabolites identified in this study could aid in TBM diagnosis.

1. Introduction

Tuberculosis meningitis (TBM) is an infectious disease of the central nervous system (CNS) caused by *Mycobacterium tuberculosis* (Mtb) and accounts for nearly 5% of all extrapulmonary tuberculosis (Gomes et al., 2014). It is associated with the highest rates of morbidity and mortality among all forms of tuberculosis in adults and children (Wilkinson et al., 2017). The outcome is often grave, involving substantial neurological sequelae or death (Chiang et al., 2014; Graham and Donald, 2014). Early diagnosis and initiation of the appropriate treatment at an optimal dose can greatly improve the clinical outcome of TBM (Török, 2015). However, there are substantial challenges in TBM diagnosis because of its variable and nonspecific clinical presentation. The definitive diagnosis of TBM mainly relies on diagnostic laboratory tests (Molicotti et al., 2014; Boehme et al., 2013), but these approaches (e.g., smear microscopy and mycobacterial cultures) do not provide rapid and accurate TBM diagnosis (Mai and Thwaites, 2017) despite numerous improvements (Chen et al., 2012a, 2012b; Fennely et al., 2012; Doern and Butler-Wu, 2016). The limited sensitivity and speed of these diagnostic approaches have led to screening for novel diagnostic markers of TBM.

Sadly, numerous attempts have failed to be translated into routine clinical care (such as antibodies against Mtb and its antigens) (Török, 2015), or been proven to have unsatisfactory sensitivity in clinical TBM diagnostic work (such as adenosine deaminase and lipoarabinomannan expression assays and interferon-γ release assays) (Pormohammad et al., 2017; Lawn et al., 2017; Yu et al., 2016). To date, only nucleic acid amplification tests (NAATs) based on detection of Mtb-specific DNA sequences in clinical specimens and cultures have shown potential to be a solution for TBM diagnosis to overcome the inadequacy of traditional diagnostic approaches (Lekhak et al., 2016). However, even Xpert MTB/RIF, a commercial cartridge-based NAAT endorsed by the World Health Organization, has been found to have highly variable sensitivity (Rufai et al., 2017; Denkinger et al., 2014; Boyles and

* Corresponding author.
E-mail address: chuili1967@126.com (L. Cui).

https://doi.org/10.1016/j.meegid.2019.01.003
Received 25 September 2018; Received in revised form 18 December 2018; Accepted 3 January 2019
Available online 04 January 2019

Table 1
The criteria of the uniform clinical case definition.

	Diagnostic criteria
Clinical entry criteria	Symptoms and signs of meningitis including one or more of the following: Headache, irritability, vomiting, fever, neck stiffness, convulsions, focal neurological deficits, altered consciousness, or lethargy
Tuberculosis meningitis classification	
Definite tuberculosis meningitis	Patients should fulfill criterion A or B: A. Clinical entry criteria plus one or more of the following: Acid-fast bacilli seen in the CSF; Mycobacterium tuberculosis cultured from the CSF; Or a CSF positive commercial nucleic acid amplification test. B. Acid-fast bacilli seen in the context of histological changes consistent with tuberculosis in the brain or spinal cord with suggestive symptoms or signs and CSF changes, or visible meningitis (on autopsy).
Probable tuberculosis meningitis	Clinical entry criteria plus a total diagnostic score of 10 or more points (when cerebral imaging is not available) or 12 or more points (when cerebral imaging is available) plus exclusion of alternative diagnoses. At least 2 points should either comme from CSF or cerebral imaging criteria.
Possible tuberculosis meningitis	Clinical entry criteria plus a total diagnostic score of 6–9 points (when cerebral imaging is not available) or 6–11 points (when cerebral imaging is available) plus exclusion of alternative diagnoses. Possible tuberculosis can not be diagnosed or excluded without doing a lumbar puncture or cerebral imaging.
Not tuberculosis meningitis	Alternative diagnosis established, without a definitive diagnosis of tuberculosis meningitis or other convincing signs of dual disease.

Thwaites, 2015). Hence, there is still an urgent need for diagnostic parameters that can accurately identify TBM.

Similar to biomacromolecules, low-molecular-weight metabolites also have the ability to diagnose diseases. In contrast to genes, mRNA, and proteins, whose functions are commonly subject to epigenetic regulation or modification, metabolites represent direct signatures of biochemical metabolic activity (Patti et al., 2012). Hence, key metabolites and related metabolic pathways that are correlated with specific human diseases have the potential to serve as biomarkers. Metabolomics, one of the omics, is an emerging approach to identify and quantify the low-molecular-weight metabolites present in a given biological system under specific conditions (Zampieri et al., 2017). Recently, it has been used to identify metabolic markers for Alzheimer's disease (Ady Enche et al., 2017), Parkinson's disease (Andersen et al., 2017), and multiple sclerosis (Bhargava and Calabresi, 2016). Nuclear magnetic resonance (NMR) spectroscopy and mass spectroscopy (MS) are the main analytical platforms of metabolomics. Although the sensitivity of NMR is lower than that of MS, NMR-based metabolomics approaches tend to have better reproducibility and stability. In addition, they do not destroy the sample, and involve simpler sample preparation procedures compared to MS-based metabolomics (Thapar and Titus, 2014; Ling et al., 2014). These characteristics make NMR-based metabolomics more suitable for the large-scale metabolic profiling of precious clinical samples than MS-based metabolomics. NMR-based metabolomics strategies have provided new tools to identify novel diagnostic markers of TBM.

At present, metabolomics research of TBM is an emerging field with only a few studies published. Due to the existence of the blood-brain barrier (BBB), some metabolic changes induced by TBM are only apparent in the cerebrospinal fluid (CSF). Although several metabolomics approaches have attempted (Mason et al., 2016b; Chatterji et al., 2016), the studies on TBM have typically used CSF as a more ideal specimen. A series of continuous CSF metabolomics studies of pediatric cases with TBM has found that Mtb infections induced a series of changes in the CSF (Mason et al., 2015; Mason et al., 2016a; Mason et al., 2017). The reason for these metabolic changes was the perturbed energy metabolism, and nitrite levels were also elevated in the CSF. Metabolic features in the CSF of pediatric cases with TBM included increased energy consumption derived from the host response to infection and elevated levels of several amino acids linked to ammonia due to increased nitrites. Compared with pediatric cases, there is little systematic information available on CSF metabolomics in adult patients with TBM, especially based on NMR platforms (Chatterji et al., 2016; Li et al., 2017; Dai et al., 2017). To date, the NMR-based metabolomics studies of the CSF of adult patients have mainly focused on discriminating between TBM and other forms of meningitis (viral or bacterial) (Chatterji et al., 2016; Li et al., 2017). These independent studies lack cross-validation and overlap due to differences in the experimental objects used. A systematic NMR-based CSF metabolomic study of TBM-containing patients in comparison with several different other forms of meningitis and meningitis-negative controls is needed to identify CSF metabolic features of TBM and screen for potential metabolic markers.

Here, we present a systematic study of CSF metabolic profiling among adult patients with TBM, VM, and BM, as well as meningitis-negative controls, using an NMR-based platform and stringent statistical analyses. Metabolic differences among TBM, bacterial and viral meningitis, and negative control samples were identified, and pathway analysis was performed. The metabolic features and potential metabolic markers were identified simultaneously. These results may aid in TBM diagnosis and improve treatment efficacy.

2. Material and methods

2.1. Sampling

Subjects with suspected TBM, VM, and BM were enrolled at the First Hospital of Jilin University, Jilin University (Changchun, China) between November 2016 and October 2017, in a specialized neurology unit that focuses on diagnosing and treating neurological diseases. In this study, CSF samples were collected from 120 subjects who completely fulfilled the inclusion and exclusion criteria. Among the 120 samples, 31, 29, 30, and 30 were collected from TBM, VM, BM, and NC subjects, respectively. TBM diagnosis was based on the uniform clinical case definition (Marais et al., 2010), and the criteria were given in Table 1. Only patients with “definite” and “probable” TBM were included in the TBM group. VM was diagnosed when a viral etiology was confirmed, or the clinical outcome was favorable with supportive and/or antiviral therapy and bacterial, fungal, and non-infectious causes of meningitis (malignancy, neurosarcoidosis, autoimmune disorders) were ruled out (Hristea et al., 2012). BM was defined as the growth of a pathogen from CSF culture or the identification of a pathogen in a CSF specimen by Gram staining, or when the clinical outcome was favorable with supportive and/or antibiotic therapy and viral, fungal, and non-infectious causes of meningitis were ruled out (Tunkel et al., 2004). The negative control (NC) group comprised patients suspected of having meningitis, but confirmed to be meningitis-negative. Exclusion criteria included age < 15 or > 70 years, > 7 days of chemotherapy or immunosuppressive therapy, current pregnancy or lactation, a history of organ transplant, and complications such as human immunodeficiency virus, cancer, diabetes, and liver or kidney disease. The study was approved by the Ethics Committee of the First Hospital of Jilin University (No. 2016-415), and was performed in accordance with the guidelines

of the Declaration of Helsinki. Written informed consent was obtained from all patients or their legal surrogates. Details regarding sample preparation are provided in the Supplementary Information.

2.2. Information of phosphate buffered saline

In our research, phosphate buffered saline (PBS) were prepared before sample preparation. The PBS contains 0.2 mol L^{-1} phosphate buffer salt, 0.2% sodium azide, 20% deuterium oxide, 0.054 mol L^{-1} potassium chloride, 2.74 mol L^{-1} sodium chloride and 1 m mol/L 3-(trimethylsilyl)propionic-2,2,3,3-d_4 acid sodium salt (TSP). TSP was used as the internal standard in ^{1}H NMR analysis, and deuterium oxide was used for a field frequency lock. Deuterium oxide, phosphate buffer salt, and TSP were purchases from Sigma-Aldrich (Darmstadt, Germany). Sodium azide used as antiseptic was purchased from Tianjin Fuchen Chemical Reagent Factory (Tianjin, China). The PBS was stored at 4 °C before used, and pH value of PBS is 7.4 at 25 °C.

2.3. Sample preparation

All CSF samples were collected from patients with suspected meningitis during a routine diagnostic workup. After centrifugation at 3000 rpm for 10 min at 4 °C, the CSF supernatant was centrifuged again at 12000 rpm for 10 min at 4 °C. Then, the supernatant was aliquoted into sterile polypropylene microtubes. All CSF sample were stored at −80 °C.

Before ^{1}H NMR analysis, CSF samples were first thawed at 4 °C. Then, thawed CSF were centrifuged at 12000 rpm for 10 min at 4 °C. Supernatant aliquots of 300 μL CSF were mixed with equal volume of PBS. The mixture was centrifuged at 12000 rpm for 10 min at 4 °C, and supernatant aliquots of 550 μL were transferred into 5 mm NMR tube (Wilmad LabGlass,Vineland, New Jersey, USA). The NMR tubes containing CSF sample were stored at 4 °C before analysis. All CSF samples were analyzed within 6 h.

2.4. Acquisition of ^{1}H NMR spectra and data processing

^{1}H NMR analyses were performed at 25 °C on a Bruker Avance III 600 (Bruker Co., Germany) spectrometer operating at a ^{1}H frequency of 600.13 MHz and equipped with a triple resonance probe. NMR spectra for CSF samples were recorded using the solvent pre-saturation pulse sequence to suppress the water signal (Wei et al., 2016). 64 transients and 64 K data points were collected with a spectral width of 6009.6 Hz, an acquisition time of 1.0224 s, a relaxation delay of 6 s. The free induction decay (FID) was zero-filled to 128 K data points, and an exponential line-broadening function of 0.3 Hz was applied to the FID prior to Fourier transformation.

All ^{1}H NMR spectra were processed using MestReNova software 6.1.0 (Mestrelab Research S.L., Spain). The phase and baseline were manually corrected to the internal standard peak (TSP) at a chemical shift of 0.0 ppm (δ0.0). Metabolomic ^{1}H NMR spectra usually span a 0.0–9.0 ppm region when scaled relative to the internal standard peak. Spectral information from endogenous metabolites is mainly concentrated in the 0.4–4.4 ppm region. The 0.0–0.4 ppm region is disturbed by TSP signals, and the 4.4–5.5 ppm region is disturbed by proton signals in water. Signals from 5.5 to 9.0 ppm are mainly attributed to medications. Because we were interested in changes in endogenous metabolites in the CSF, only signals from 0.4 to 4.4 ppm were investigated. The spectra in this range were divided in to 400 0.01 ppm-wide segments. Data for each sample were normalized to the total area to correct for the ^{1}H NMR response shift.

2.5. Multivariate statistical analysis

Multivariate statistical analysis of the pretreated NMR data was performed using the statistical software package SIMCA 14.1 (Umetrics, Sweden). Unsupervised principal component analysis (PCA) and Hotelling's T^2 test were used to remove case outliers for each experimental group; assessment of overall variance was used to remove variable outliers. Supervised orthogonal signal correction-partial least squares-discriminant analysis (OPLS-DA) was subsequently performed to identify important variables. Three parameters (R^2X, R^2Y, and Q^2) were used to evaluate the reliability of the established OPLS-DA models. These parameters were calculated by cross-validation according to the default settings. R^2X and R^2Y indicated the goodness of fit, and Q^2 indicated the predictability of the model. The permutation test was performed 200 times to validate the OPLS-DA model, and the results of the permutation test included R^2 and Q^2 values. R^2 is the explained variance, and Q^2 is the predictive ability of the model. The variable importance in the projection (VIP) of all peaks from OPLS-DA models was used as a coefficient for chemical shift selection, and variables with a VIP value > 1.0 were considered contributors to group discrimination. Univariate statistical analysis (p value < .05) was used to detect significant differences between the TBM group and other groups in the chemical shifts of each metabolite. Chemical shifts with VIP > 1.0 and p < .05 were considered significant. Corresponding metabolites were identified according to the spectra of standards in the Human Metabolome Database (http://www.hmdb.ca/) and previously published reports.

2.6. Pathway analysis

MetabolAnalyst 4.0 (http://www.metaboanalyst.ca/MetaboAnalyst/) was used to perform pathway analysis and visualization of all chemical metabolites present at different levels in TBM, VM, BM, and NC CSF samples (Xia et al., 2015). Metabolite set enrichment analysis (MSEA) using over representation analysis (ORA) algorithms was performed with a pathway-associated metabolite set library that contained 99 metabolite sets based on normal metabolic pathways to identify biologically meaningful patterns significantly enriched in quantitative metabolomics (Xia and Wishart, 2010).

2.7. Univariate statistical analysis

Data on subjects were analyzed using SPSS 17.0 (IBM, USA). Student's t-test (p < .05) was used to detect significant differences between the TBM group and other groups in the chemical shifts of each metabolite. Distributed continuous variables were presented as the mean ± standard deviation (SD). Distributed continuous variables were also compared using Student's t-test. Categorical variables were compared using Fisher's exact test. All tests were two-sided and p < .05 was considered statistically significant (Fig. 1).

3. Results

3.1. Characteristics of the sample population

After PCA analysis and Hotelling's T^2 test, the total number of CSF samples was reduced to 100, including 25, 27, 20, and 28 from TBM, VM, BM, and NC subjects, respectively. Patient demographic information is summarized in Table 2, and laboratory test results and clinical symptom of patients with TBM, VM and BM are summarized in Table 3.

3.2. ^{1}H NMR spectra of CSF samples

Changes of endogenous metabolites were observed when the TBM group was compared with the VM, BM, and NC groups. Typical NMR spectra from each group, spanning the 0.4–4.4 ppm region, are shown in Fig. 2, and spectrum resonances assigned to various metabolites are noted (Supplementary Table S2).

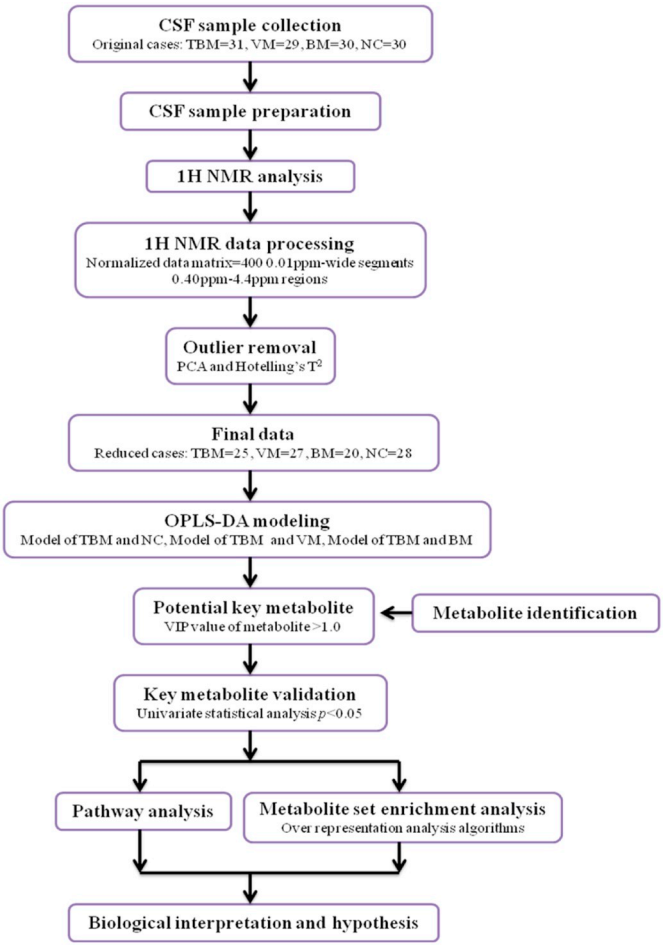

Fig. 1. Stepwise work flow chart of the research.

Table 2
Demographic characteristics of the participants.

Characteristics	TBM[a]	VM[b]	BM[c]	NC[d]
Sample size	25	27	20	28
Age(years)[e]	36.1 ± 12.2	36.3 ± 17.1	41.1 ± 12.8	39.9 ± 14.9
Gender(male/female)	14/11	15/12	12/8	13/15

[a] TBM, tuberculosis meningitis.
[b] VM, viral meningitis.
[c] BM, bacterial meningitis.
[d] NC, negative control.
[e] Ages are presented as the mean ± SD.

3.3. Data analysis and identification of important metabolites

As ethanol is a contamination during lumber puncture, the signal of ethanol should be removed during multivariate analysis. In order to ensure the accuracy of the analysis results, unsupervised PCA analysis and Hotelling's T^2 test, with a confidence level of 95%, was used to remove case outliers. The TBM data tended to separate from the data of the other groups, but this trend was not as obvious between the TBM and BM groups. To improve the separation and identify metabolic differences, supervised OPLS-DA analysis was performed to establish OPLS-DA analysis models of the TBM and NC, TBM and VM, and TBM and BM sample data (Fig. 3). Metabolic differences between the TBM group and the other three groups were visualized using score plots of the three OPLS-DA models, which suggested that the CSF metabolic profiling of TBM was significantly different from that of the other groups. The contribution of different variables to the discriminating ability of each OPLS-DA model is shown in the corresponding plots. The degree of contribution of each variable was expressed as a VIP value (Fig. 4). Variables with higher VIP values deviated farther from the origin in the loading plot.

Table 3
Clinical presentations, laboratory characteristic of the patients with TBM, VM, and BM.

	TBM[a] (n = 25)	VM[b] (n = 27)	BM[c] (n = 20)
Cerebrospinal fluid			
Protein (g/L)	2.53 ± 1.02	0.52 ± 0.15	2.36 ± 1.50
Glucose (m mol/L)	1.94 ± 0.81	3.26 ± 0.51	1.84 ± 0.88
Chloride (m mol/l)	111.77 ± 8.04	125.06 ± 2.63	122.55 ± 6.32
WBC[d] ($\times 10^6$/L)	230 (51–510)	132 (11–528)	4348 (349–15,146)
Monocyte predominance	23/25 (92.0%)	23/27 (85.2%)	5/20 (25.0%)
Clinical sign and symptom			
Headache	22/25 (88.0%)	23/27 (85.2%)	17/20 (85.0%)
Fever	24/25 (96.0%)	25/27 (92.6%)	19/20 (95.0%)
Vomiting	19/25 (76.0%)	20/27 (74.0%)	17/20 (85.0%)
Convulsions	6/25 (24.0%)	5/27 (18.5%)	3/20 (15.0%)
Altered consciousness	8/25 (32.0%)	7/27 (25.9%)	6/20 (30.0%)
Meningeal irritation	21/25 (84.0%)	23/27 (85.2%)	17/20 (85.0%)

[a] TBM, tuberculosis meningitis.
[b] VM, viral meningitis.
[c] BM, bacterial meningitis.
[d] WBC, White blood cell count.

Permutation tests were used to validate the constructed OPLS-DA models, and the reliability of models was represented by the predicted variation, Q^2, and the explained variation, R^2, calculated by cross-validation. In three OPLS-DA models, the values of R^2 and Q^2 were above 0.5, suggesting that these three model is both good and reliable (Table 4). The Q^2 value of the model between TBM and BM was a little lower than the Q^2 values of the other two models, suggesting that the predictive ability of the OPLS-DA model between TBM and BM was a little weaker. One reason for this may be the wide range of concentrations of the same metabolites in the BM group, due to patient-to-patient variations in the stage of disease progression and the specific bacterial pathogen causing the infection.

Metabolites were identified based on chemical shifts. Only metabolites with VIP > 1.0 and $p < .05$ were considered potential metabolic markers (Table 5, Table 6, and Table 7). The important metabolites included several carbohydrate metabolites, amino acids, lipid metabolites, nucleoside metabolites and other metabolites.

3.4. Metabolic differences between TBM and NC CSF

21 metabolites were identified to be potential metabolic markers between the TBM and NC groups. The VIP and p values of these metabolites are shown in Table 5. These important metabolites included several carbohydrate metabolites (glucose, lactate, and *myo*-inositol), amino acids (L-alanine, L-isoleucine, and glycine), lipid metabolites (choline, 3-hydroxy isovalerate, and caprate), nucleoside metabolites (1,3-dimethyluric acid) and metabolites derived from microorganisms (cyclohexane and isobutyrate). Consistent with the results of several reports (Thwaites et al., 2003; Donald and Malan, 1985), increased level of lactate in the CSF of patients with TBM has been observed in our research. Lactate may be the potential biomarkers of TBM diagnosis based on results of our research and the studies published before. Besides, amino acids may be another series of potential biomarkers. Changes in concentrations of amino acids caused by TBM have been reported by several studies (Li et al., 2017; Qureshi et al., 1998; Corston et al., 1981). The changes of amino acids have also been observed in our research. Although there was not a uniform conclusion about the change trends of amino acids, it was sure that TBM can cause changes in

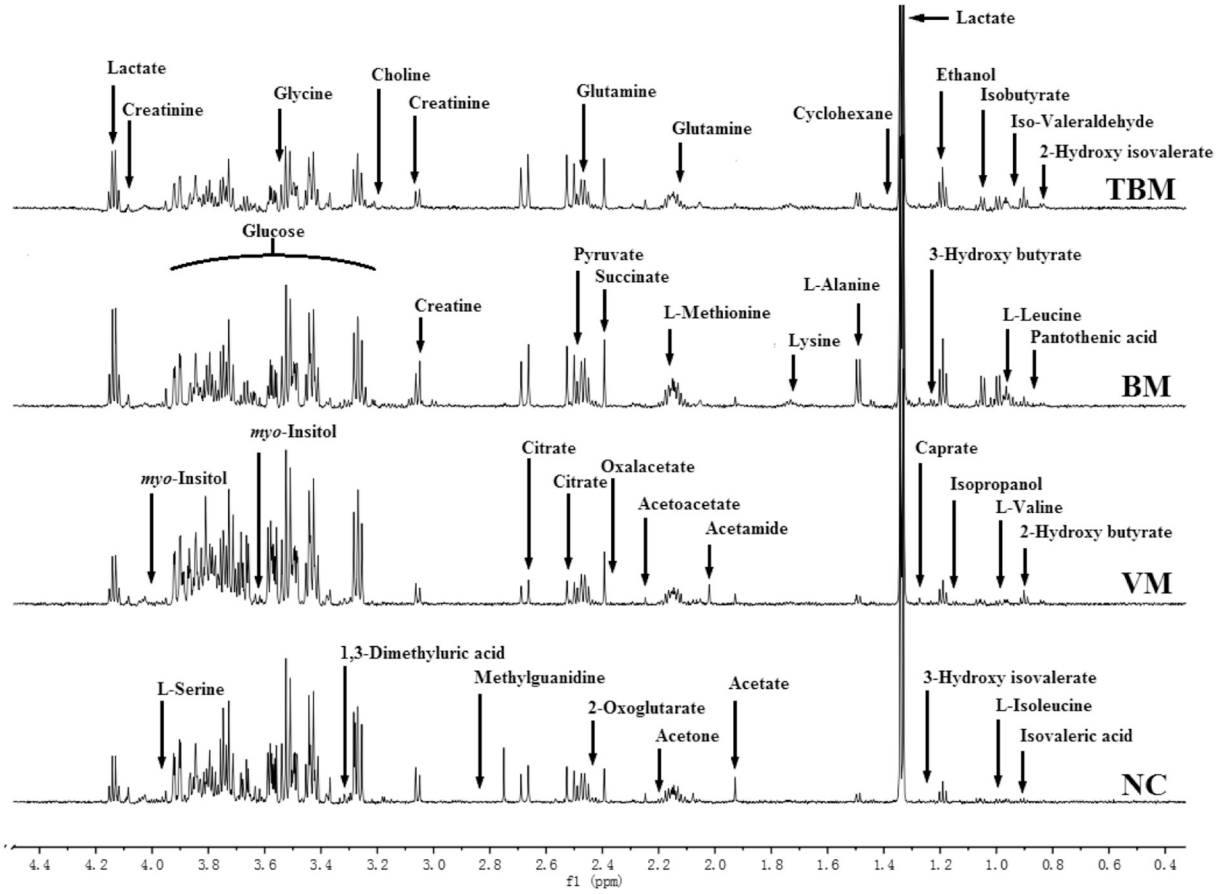

Fig. 2. Typical ^{1}H NMR spectra of CSF samples (NC, VM, BM and TBM).

amino acid concentration in CSF. Levels of amino acids or their metabolites in CSF were related to the Mtb-induced infection in CNS, but further research is needed. Some researches have suggested that additional energy requirement was the cause of these metabolic changes (Mason et al., 2015; Rodríguez-Núñez et al., 1993). Pathway analysis showed that pyruvate metabolism, glycine, serine and threonine metabolism, citrate cycle (TCA cycle), and glycolysis or gluconeogenesis were the four top-ranking impacted canonical KEGG pathways (Table 8 and Fig. 5). Over-representation analysis in pathway-associated metabolite sets indicated that some pathways including glucose-alanine cycle, alanine metabolism, and gluconeogenesis were over-represented in the CSF of patients with TBM compared to meningitis-negative controls (Fig. 5). The results of pathway analysis and over-representation analysis have indicated that the CSF metabolic differences between TBM and NC groups were mainly involved in amino acid and carbohydrate metabolism. These results also suggested that the perturbed energy metabolism is the key characteristics in the brain of patients with TBM, and the disturbances of amino acid metabolism may be another metabolic feature in the CSF of patients with TBM.

3.5. Metabolic differences between TBM and VM CSF

23 metabolites were identified to be potential metabolic markers between the TBM and VM groups. The VIP and *p* values of these metabolites are shown in Table 6. 18 of these metabolites were same to the metabolic markers between TBM and NC groups. These overlapped metabolites included several carbohydrate metabolites (glucose, lactate, and *myo*-inositol), amino acids (L-alanine, and L-isoleucine), lipid metabolites (3-hydroxy isovalerate, and caprate), nucleoside metabolites (1,3-dimethyluric acid) and metabolites derived from microorganisms (cyclohexane and isobutyrate). These same metabolic markers have suggested that metabolic differences between TBM and VM were similar to those between TBM and NC. The patients with TBM have a more perturbed energy metabolism in brain than patients with VM. Compared with the metabolic differences between TBM and NC groups, the main differences between TBM and VM groups were the identification of more amino acids, namely L-valine, L-leucine, L-isoleucine, L-alanine, and L-serine. Pathway analysis showed that pyruvate metabolism, glycine, serine and threonine metabolism, citrate cycle (TCA cycle), and alanine, aspartate and glutamate metabolism were the four top-ranking impacted canonical KEGG pathways (Table 8 and Fig. 5). Over-representation analysis in pathway-associated metabolite sets indicated that some pathways including glucose-alanine cycle, phosphatidylethanolamine biosynthesis, and valine, leucine and isoleucine degradation were over-represented in the CSF of patients with TBM compared to the patients with VM. All these results of pathway analysis and over-representation analysis have indicated that TBM may induce more perturbations in amino acid metabolism and carbohydrate metabolism in brain than VM.

3.6. Metabolic differences between TBM and BM CSF

Only six metabolites were significantly different between TBM and BM groups, including L-valine, L-serine, 1,3-dimethyluric acid, lysine, acetamide, and L-alanine. The VIP and *p* values of these metabolites are shown in Table 7. The amount of metabolic markers between TBM and BM groups were less than that between TBM and VM groups and between TBM and NC groups. Four of the metabolic markers were amino acids, while the differences of carbohydrate metabolism between TBM and BM groups were not obvious based on our results. The results of pathway analysis also showed that the top-ranking impacted canonical KEGG pathways were all amino acid metabolism pathways (Table 8 and

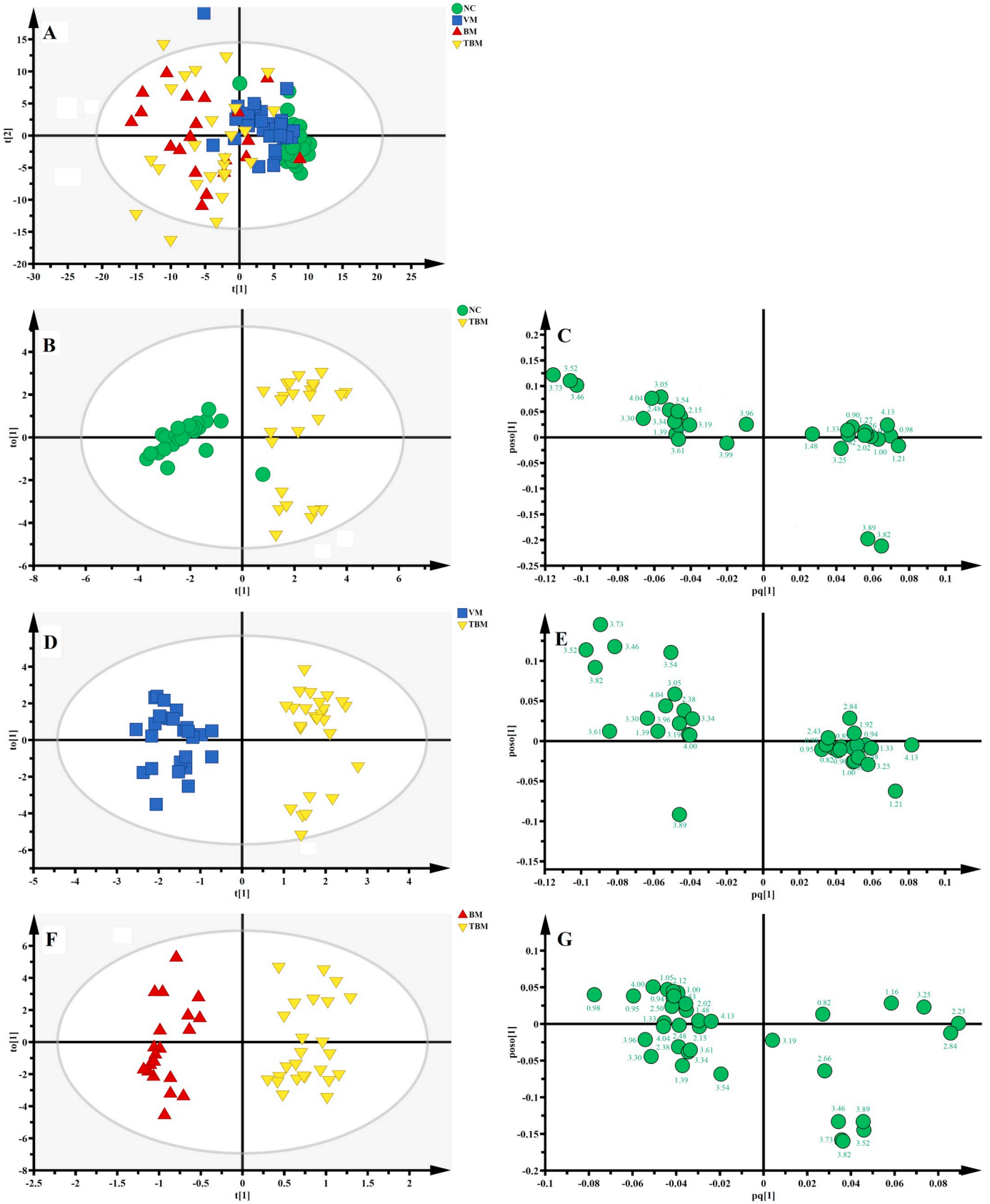

Fig. 3. Multivariate statistical analysis of ^{1}H NMR spectra of CSF samples. (A) Score plot of the PCA model based on the finial participants. (B) Score plot of the OPLS-DA model between TBM and NC groups. (C) Corresponding loading plot of the OPLS-DA model of TBM and NC groups. (D) Score plot of the OPLS-DA model of TBM and VM groups. (E) Corresponding loading plot of the OPLS-DA model of TBM and VM groups. (F) Score plot of the OPLS-DA model of TBM and VM groups. (G) Corresponding loading plot of the OPLS-DA model of TBM and BM groups.

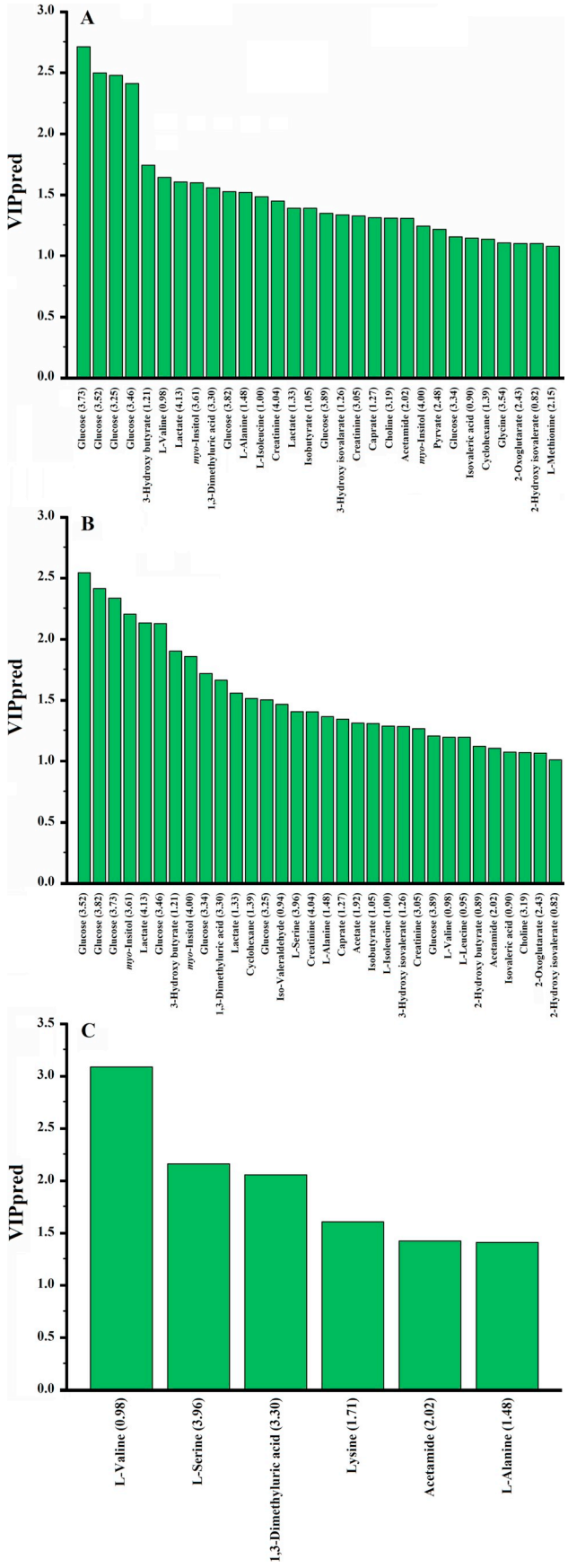

Fig. 4. VIP plot of key metabolites.(A) VIP plot of key metabolites between TBM and NC groups. (B) VIP plot of key metabolites between TBM and VM groups. (C) VIP plot of key metabolites between TBM and BM groups.

Table 4
R^2 and Q^2 values of the PCA models and three OPLS-DA models.

	R^2X(cum)	R^2Y(cum)	Q^2(cum)
PCA	0.567		0.320
OPLS-DA of TBM and NC	0.628	0.867	0.764
OPLS-DA of TBM and VM	0.646	0.922	0.715
OPLS-DA of TBM and BM	0.633	0.890	0.623

Table 5
Key metabolites that discriminate TBM and NC groups.

	Metabolites	Chemical Shift (ppm)	VIP[a]	*p*-Value[b]	FC[c]	Trend[d]
1	Glucose	3.25	2.475	0.004	0.40	↓
		3.34	1.151	< 0.001	0.35	↓
		3.46	2.407	< 0.001	0.47	↓
		3.52	2.493	< 0.001	0.43	↓
		3.73	2.709	< 0.001	0.45	↓
		3.82	1.522	0.004	0.44	↓
		3.89	1.344	0.005	0.47	↓
2	3-Hydroxy butyrate	1.21	1.739	0.002	2.08	↑
3	L-Valine	0.98	1.637	< 0.001	4.89	↑
4	*myo*-Insitol	3.60	1.595	0.002	0.43	↓
		4.00	1.239	0.005	0.42	↓
5	1,3-Dimethyluric acid	3.30	1.553	< 0.001	0.57	↓
6	L-Alanine	1.48	1.515	< 0.001	2.93	↑
7	L-Isoleucine	1.00	1.480	< 0.001	3.01	↑
8	Lactate	1.33	1.386	0.004	4.41	↑
		4.13	1.601	< 0.001	4.04	↑
9	Isobutyrate	1.05	1.386	0.001	3.19	↑
10	3-Hydroxy isovalerate	1.26	1.331	< 0.001	3.30	↑
11	Creatinine	3.05	1.322	< 0.001	0.81	↓
		4.04	1.444	0.003	0.80	↓
12	Caprate	1.27	1.308	< 0.001	2.97	↑
13	Choline	3.19	1.305	0.012	0.48	↓
14	Acetamide	2.02	1.303	< 0.001	2.21	↑
15	Pyruvate	2.48	1.212	0.003	0.79	↓
16	Isovaleric acid	0.90	1.139	< 0.001	2.06	↑
17	Cyclohexane	1.39	1.131	0.001	0.77	↓
18	Glycine	3.54	1.101	0.017	0.70	↓
19	2-Oxoglutarate	2.43	1.096	0.001	1.56	↑
20	2-Hydroxy isovalerate	0.82	1.095	< 0.001	2.91	↑
21	L-Methionine	2.15	1.072	0.007	0.83	↓

[a] VIP, variable importance in the projection. Values (cut-off threshold 1.0) were obtained from the OPLS-DA model.
[b] p-Value were calculated using the Student's *t*-test.
[c] FC, fold change. Values > 1.0 indicate that levels were higher in the CSF of TBM patients; values < 1.0 indicate that levels were lower in the CSF of TBM patients.
[d] "↑" indicate that the levels were higher in the CSF of TBM patients; "↓" indicate that levels were lower in the CSF of TBM patients.

Fig. 5), indicating that the significant differences between TBM and BM were amino acid profiles in CSF. In addition, different from the situation between TBM and VM groups and between TBM and NC groups, levels of all these four amino acids were lower in the CSF of patients with TBM than those in the CSF of patients with BM. Based on these results, patients with BM may have more disturbances in amino acid metabolism than patients with TBM. Over-representation analysis in pathway-associated metabolite sets indicated that some amino acid metabolism pathways such as glycine and serine metabolism were over-represented in the CSF of patients with BM compared to the patients with TBM (Fig. 5).

Table 6
Key metabolites that discriminate TBM and VM groups.

	Metabolites	Chemical Shift (ppm)	VIP[a]	*p*-Value[b]	FC[c]	Trend[d]
1	Glucose	3.25	1.498	0.002	0.61	↓
		3.34	1.713	0.003	0.62	↓
		3.46	2.123	< 0.001	0.58	↓
		3.52	2.539	< 0.001	0.57	↓
		3.73	2.331	< 0.001	0.60	↓
		3.82	2.410	< 0.001	0.58	↓
		3.89	1.201	0.006	0.64	↓
2	*myo*-Insitol	3.60	2.200	< 0.001	0.72	↓
		4.00	1.853	0.012	0.75	↓
3	3-Hydroxy butyrate	1.21	1.897	0.007	1.97	↑
4	1,3-Dimethyluric acid	3.30	1.660	< 0.001	0.65	↓
5	Lactate	1.33	1.554	0.008	3.08	↑
		4.13	2.129	< 0.001	3.10	↑
6	Cyclohexane	1.39	1.510	0.001	0.77	↓
7	Iso-Valeraldehyde	0.94	1.461	0.002	1.64	↑
8	L-Serine	3.96	1.402	0.001	0.75	↓
9	L-Alanine	1.48	1.362	0.003	3.47	↑
10	Caprate	1.27	1.340	< 0.001	2.04	↑
11	Acetate	1.92	1.309	0.024	2.38	↑
12	Isobutyrate	1.05	1.305	0.009	2.07	↑
13	L-Isoleucine	1.00	1.283	0.003	1.98	↑
14	3-Hydroxy isovalerate	1.26	1.280	< 0.001	1.89	↑
15	Creatinine	3.05	1.262	0.006	0.88	↓
		4.04	1.401	0.004	0.86	↓
16	L-Valine	0.98	1.191	0.036	2.90	↑
17	L-Leucine	0.95	1.191	0.003	2.77	↑
18	2-Hydroxy butyrate	0.89	1.117	0.007	1.57	↑
19	Acetamide	2.02	1.100	< 0.001	1.32	↑
20	Isovaleric acid	0.90	1.070	0.027	1.50	↑
21	Choline	3.19	1.065	< 0.001	0.82	↓
22	2-Oxoglutarate	2.43	1.061	0.003	1.48	↑
23	2-Hydroxy isovalerate	0.82	1.005	0.001	1.83	↑

[a] VIP, variable importance in the projection. Values (cut-off threshold 1.0) were obtained from the OPLS-DA model.
[b] p-Value were calculated using the Student's *t*-test.
[c] FC, fold change. Values > 1.0 indicate that levels were higher in the CSF of TBM patients; values < 1.0 indicate that levels were lower in the CSF of TBM patients.
[d] "↑" indicate that the levels were higher in the CSF of TBM patients; "↓" indicate that levels were lower in the CSF of TBM patients.

Table 7
Key metabolites that discriminate TBM and BM groups.

	Metabolites	Chemical Shift (ppm)	VIP[a]	*p*-Value[b]	FC[c]	Trend[d]
1	L-Valine	0.98	3.081	0.004	0.55	↓
2	L-Serine	3.96	2.155	0.004	0.52	↓
3	1,3-Dimethyluric acid	3.30	2.050	0.010	0.68	↓
4	Lysine	1.71	1.602	0.011	0.49	↓
5	Acetamide	2.02	1.418	0.008	0.49	↓
6	L-Alanine	1.48	1.403	0.005	0.58	↓

[a] VIP, variable importance in the projection. Values (cut-off threshold 1.0) were obtained from the OPLS-DA model.
[b] p-Value were calculated using the Student's *t*-test.
[c] FC, fold change. Values > 1.0 indicate that levels were higher in the CSF of TBM patients; values < 1.0 indicate that levels were lower in the CSF of TBM patients.
[d] "↑" indicate that the levels were higher in the CSF of TBM patients; "↓" indicate that levels were lower in the CSF of TBM patients.

4. Discussion

4.1. Metabolic differences between TBM and NC CSF

Mtb infection induced a series of metabolic changes in the CSF, and several metabolites were identified that could be valuable in discriminating between TBM and NC samples (Table 5). Previous research has indicated that changes in CSF metabolites in TBM are related to perturbed energy metabolism in the brain (Mason et al., 2015).

Because carbohydrate metabolism is a direct energy source for the CNS, metabolic changes involved in carbohydrate metabolism were evident, including increased lactate levels and reduced glucose levels (Table 5 and Table 8) (Mason et al., 2016a; Thwaites et al., 2003; Bang et al., 2016). These changes are consistent with many previous reports, and are classic metabolic features of TBM caused by increased energy demand in response to Mtb infection, and resulting in increased glucose catabolism through glycolysis. Lactate and glucose concentrations are related to the progression and prognosis of TBM, and lactate has been suggested as a useful TBM biomarker (Török, 2015). Moreover, the level of D-lactate is greater than that of L-lactate in the CSF of adult patients with TBM (Chen et al., 2012a, 2012b), while only L-lactate has been observed in the CSF of pediatric patients with TBM (Mason et al., 2016a). In the CSF of patients with TBM, the L enantiomer of lactate is considered to be the response from the host to the infection, while D-form is derived from the metabolism of Mtb itself. The researches on the chirality of lactate suggest that the reasons of increased energy requirements in adult and pediatric patients are different. In addition, the consumption of glucose induces a decrease in the level of *myo*-inositol, a bound component of phospholipids and inositol phosphate derivatives that play an important role in various metabolic processes, and is produced in sufficient amounts by the human body from D-glucose (Croze and Soulage, 2013). Levels of lactate and glucose might potentially be used to evaluate the prognosis of TBM.

Perturbed energy metabolism in the brain causes changes in not only carbohydrate metabolism but also amino acid metabolism (Table 8). Thus, the amino acids and the metabolites involved in amino acid metabolism that showed significantly changed levels also have the ability to serve as metabolic markers of TBM. Half of the identified metabolites were involved in amino acid metabolism, indicating that these changes are another metabolic feature of patients with TBM. The concentrations of four amino acids, namely L-alanine, L-isoleucine, and glycine, were significantly changed in the CSF of the TBM group compared with the NC group. L-isoleucine and L-alanine levels were increased in the CSF of TBM patients. L-isoleucine, a branched chain amino acid (BAAC), participates directly or indirectly in a variety of important biochemical functions in the CNS, such as providing building blocks for energy production through gluconeogenesis (Sperringer et al., 2017). L-alanine is the amino acid most closely related to carbohydrate metabolism, as it can be directly converted to pyruvate (Mason et al., 2017). Decreases were observed in the glycine, and L-methionine levels. Glycine, an inhibitory neurotransmitter, is a precursor of sarcosine during glycine, serine, and threonine metabolism. Choline is also involved in glycine, serine, and threonine metabolism, and its final product is also sarcosine. Decreases in glycine and choline levels may serve to maintain the sarcosine balance in the CSF. L-Methionine is a sulfur-containing amino acid, and is known as a building block of protein. It is also a major source of methyl groups in diverse methyl-transferring reactions, and its cofactor, S-adenosyl methionine (SAM), is the main cellular carrier of methyl groups (Shim et al., 2017). Increased methyl-transferring reactions and protein biosynthesis may be the reason of the reduced L-methionine level. Metabolic changes in CSF amino acid metabolism induced by TBM have been previously reported. However, although our results partially overlap with those of previous studies, some of the changes observed differed between

Table 8
Pathway analysis of key metabolites.

	Pathway name	Total[a]	Hits[b]	Raw p[c]	FDR[d]	Impact[e]
TBM vs NC	Pyruvate metabolism	32	2	0.020567	0.1266	0.32010
	Glycine, serine and threonine metabolism	48	3	0.004160	0.0555	0.18774
	Citrate cycle (TCA cycle)	20	2	0.008280	0.0736	0.17601
	Glycolysis or Gluconeogenesis	31	3	0.001165	0.0233	0.09530
	Butanoate metabolism	40	3	0.002461	0.0394	0.08996
	Alanine, aspartate and glutamate metabolism	24	3	0.000541	0.0206	0.05698
	Cysteine and methionine metabolism	56	3	0.006438	0.0736	0.05455
	Taurine and hypotaurine metabolism	20	2	0.008280	0.0736	0.05395
	Valine, leucine and isoleucine biosynthesis	27	3	0.000771	0.0206	0.04823
	Vitamin B6 metabolism	32	2	0.020567	0.1266	0.03828
	Glycerophospholipid metabolism	39	1	0.243190	0.6507	0.02120
	Starch and sucrose metabolism	50	1	0.300970	0.6507	0.01703
	Ascorbate and aldarate metabolism	45	2	0.038904	0.1945	0.01617
	Primary bile acid biosynthesis	47	1	0.285640	0.6507	0.00822
	Arginine and proline metabolism	77	2	0.100820	0.4033	0.00645
	Galactose metabolism	41	1	0.254020	0.6507	0.00276
TBM vs VM	Pyruvate metabolism	32	2	0.025436	0.2035	0.23703
	Glycine, serine and threonine metabolism	48	2	0.053683	0.3304	0.13604
	Citrate cycle (TCA cycle)	20	1	0.147120	0.6923	0.08577
	Alanine, aspartate and glutamate metabolism	24	2	0.014695	0.1306	0.05698
	Aminoacyl-tRNA biosynthesis	75	5	0.000212	0.0170	0.05634
	Valine, leucine and isoleucine biosynthesis	27	3	0.001083	0.0433	0.03975
	Sulfur metabolism	18	2	0.008379	0.1117	0.03307
	Taurine and hypotaurine metabolism	20	2	0.010308	0.1178	0.03237
	Valine, leucine and isoleucine degradation	40	3	0.003427	0.0548	0.02232
	Glycerophospholipid metabolism	39	1	0.267690	0.8798	0.02120
	Vitamin B6 metabolism	32	1	0.225280	0.8192	0.01914
	Methane metabolism	34	1	0.237630	0.8265	0.01751
	Starch and sucrose metabolism	50	1	0.329920	0.8798	0.01703
	Cysteine and methionine metabolism	56	2	0.070614	0.4035	0.01197
	Arginine and proline metabolism	77	1	0.462110	1.0000	0.00645
	Butanoate metabolism	40	2	0.038532	0.2802	0.00480
	Selenoamino acid metabolism	22	2	0.012415	0.1242	0.00321
	Galactose metabolism	41	1	0.279400	0.8798	0.00276
	Glycolysis or Gluconeogenesis	31	3	0.001631	0.0435	0.00046
TBM vs BM	Lysine degradation	47	1	0.093968	0.4512	0.14675
	Glycine, serine and threonine metabolism	48	1	0.095887	0.4512	0.13604
	Aminoacyl-tRNA biosynthesis	75	4	0.000004	0.0003	0.11268
	Lysine biosynthesis	32	1	0.064781	0.4039	0.09993
	Alanine, aspartate and glutamate metabolism	24	1	0.048910	0.3992	0.05698
	Taurine and hypotaurine metabolism	20	1	0.040894	0.3992	0.03237
	Methane metabolism	34	1	0.068716	0.4039	0.01751
	Valine, leucine and isoleucine biosynthesis	27	1	0.054887	0.3992	0.01325
	Cysteine and methionine metabolism	56	2	0.005084	0.2033	0.01197

[a] Total, total number of compounds in the pathway.
[b] Hits, the number of compounds that match with our experimental data.
[c] Raw p, original p value calculated from the enrichment analysis.
[d] FDR, False Discovery Rate.
[e] Impact, pathway impact value calculated from pathway topology analysis.

studies (Li et al., 2017; Qureshi et al., 1998; Corston et al., 1981). Differences in disease progression and measurement methods may have caused these discrepancies.

Some identified metabolites indicated that Mtb infection also affected CSF lipid and nucleoside metabolism. For instance, levels of three fatty acids, i.e., isovaleric acid, 3-hydroxy isovalerate, and caprate, were increased in the CSF of patients with TBM. A derivative of purine, 1,3-dimethyluric acid, also showed altered levels. In addition, some metabolites, including cyclohexane and isobutyrate, indicated the presence of microorganisms. According to the Kyoto Encyclopedia of Genes and Genomes (http://www.kegg.jp/), these two compounds may be microbial metabolites. Cyclohexane is derived from caprolactam degradation, and isobutyrate is derived from the degradation of aromatic compounds.

4.2. Metabolic differences between TBM and VM CSF

The real difficulty in TBM diagnosis is distinguishing it from VM. The clinical characteristics of the CSF, such as clear appearance, negative culture for typical bacterial pathogens, normal white blood cell count, and pleocytosis with mononuclear predominance, are similar in patients with TBM and VM (Hristea et al., 2012; Bahr and Boulware, 2014). Consistent with previous research, we found that the metabolic profiles of the CSF of patients with TBM and VM were quite different (Table 6). The differences observed were similar to those between the TBM and NC groups, including the lactate and glucose trends, indicating that TBM induces higher energy demands than VM. In addition, three fatty acids, i.e., isovaleric acid, 3-hydroxy isovalerate, and caprate, showed the same trends as observed between the TBM and NC groups.

Previous studies found that the CSF amino acid levels in patients with TBM and VM were different (Li et al., 2017; Qureshi et al., 1998; Corston et al., 1981). We also observed differences in amino acid levels, although the results were not fully consistent with previous reports. Compared with the differences between the TBM and NC groups, more amino acids changed significantly between the TBM and VM groups. The concentrations of five amino acids were different, including L-valine, L-leucine, L-isoleucine, L-alanine, and L-serine. Similar to the NC

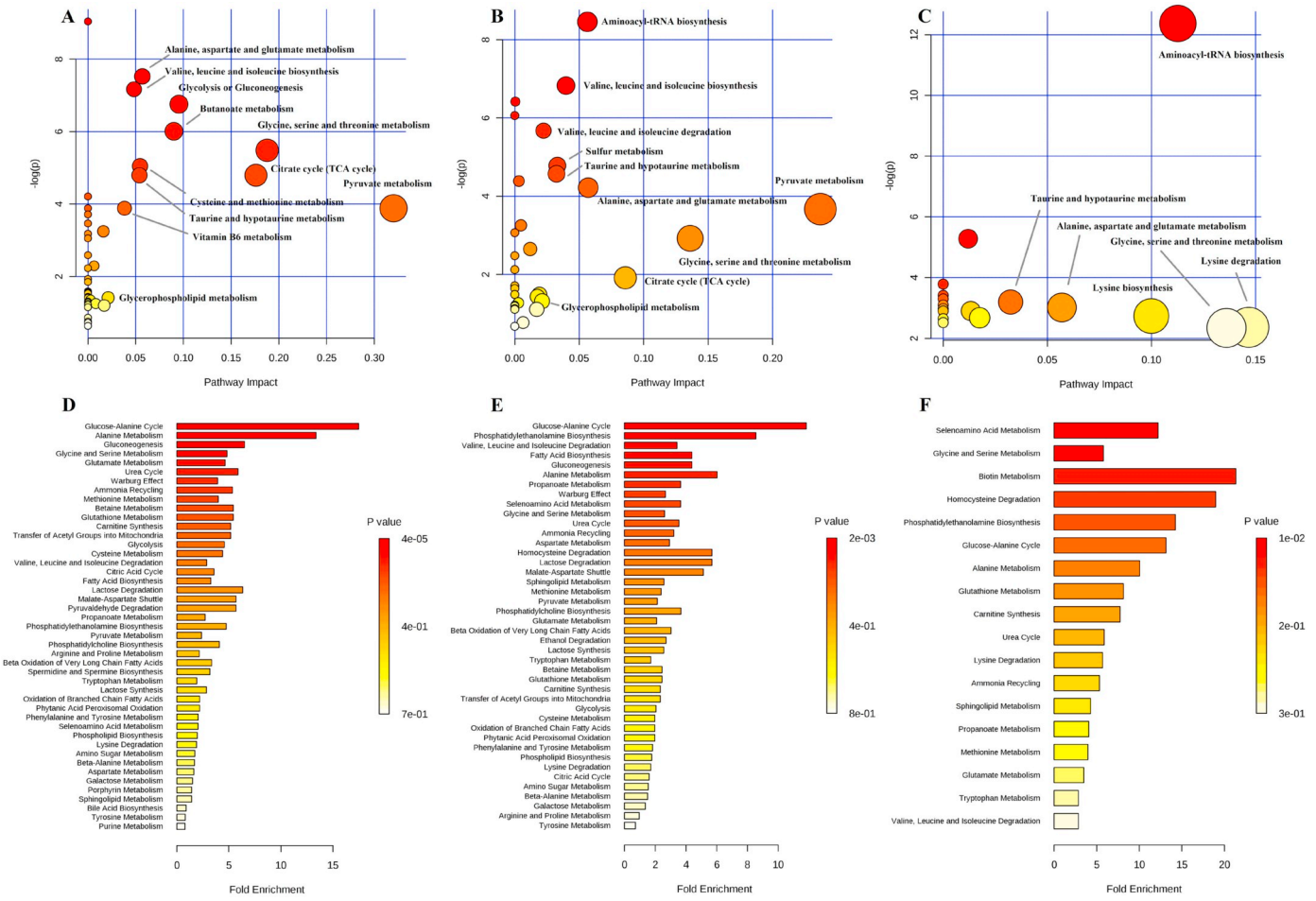

Fig. 5. Pathway analysis and enrichment analysis of key metabolites in CSF samples. Pathway named in the figure had an impact > 0.02. (A) Pathway analysis of key metabolites in CSF samples from TBM and NC groups. (B) Pathway analysis of key metabolites in CSF samples from TBM and VM groups. (C) Pathway analysis of key metabolites in CSF samples from TBM and BM groups. (D) Enrichment analysis of key metabolites in CSF samples from TBM and NC groups. (E) Enrichment analysis of key metabolites in CSF samples from TBM and VM groups. (F) Enrichment analysis of key metabolites in CSF samples from TBM and BM groups.

comparison, BAAC (L-valine, L-leucine, and L-isoleucine) and L-alanine levels were increased in the CSF of patients with TBM, whereas the levels of the other amino acids decreased, as did those of metabolites of glycine, serine, and threonine metabolism. Acetamide was elevated in the CSF of the TBM group compared with the VM and NC groups. Acetamide is the product of acetate and ammonia, and is derived from the degradation of amino acids. Increased acetamide levels suggest that amino acid degradation has increased, and that nitrogen metabolism is disturbed in the CSF of patients with TBM. Decreased creatinine levels were also observed in the CSF of the TBM group compared with the VM and NC groups. Because creatinine is produced fairly constantly during homeostasis and has a slow diffusion rate across the BBB, its decrease in TBM may be linked to the progression of neuronal injury and BBB disruption (Mason et al., 2015).

Taken together, these metabolic differences suggest that the CSF metabolic profiles of TBM and VM are different, and that CSF metabolomics can provide new diagnostic parameters to differentiate between these two forms of meningitis. Additionally, the difference in metabolites between the TBM and VM groups has the potential to differentiate TBM patients from VM patients.

4.3. Metabolic differences between TBM and BM CSF

There were 26 metabolites that contributed to discriminating between TBM and BM patients in the OPLS-DA analysis, but only six of them were proved to be significantly different (Supplementary Table S3 and Table 7). Despite their limited amount, the metabolites identified still had the ability to distinguish between the TBM and BM groups. Levels of some classic metabolic markers of TBM, such as lactate, glucose, and creatinine, were found to be not significant different between TBM and BM groups. Increased lactate has been observed in CSF of patients with BM (Sanaei Dashti et al., 2017; Giulieri et al., 2015), but it could not be used as a metabolic marker to distinguish BM from TBM based on our results. The similar levels of lactate and glucose have suggested that the additional energy demand in brain was not only the classic metabolic characteristics of TBM, but also the metabolic characteristics of BM. In addition, the progression of neuronal injury and BBB disruption of patients with TBM and BM may be similar based on the similar change trend in creatinine.

The amino acid metabolism was more disturbed in the CSF of patients with BM than that in the CSF of patients with TBM. Four of the six key metabolites were amino acids (L-valine, L-serine, lysine, and L-alanine), and the levels of these amino acids were higher in the CSF of patients with BM than those in the CSF of patients with TBM. As the product of acetate and ammonia, increased acetamide levels suggest that there is a more disturbed nitrogen metabolism in BM group than that in TBM group. Because amino acid degradation is one of the main source of ammonia in vivo, the disturbed nitrogen metabolism may be caused by the elevated amino acid degradation.

5. Conclusion

In this study, we performed systematic metabolic profiling of TBM, VM, BM, and meningitis-negative CSF samples, and demonstrated that ^{1}H NMR-based metabolomics can distinguish TBM from other groups with high reliability. Several metabolites were identified, which represent potential metabolic biomarkers for discriminating among patients with TBM, VM, and BM, as well as meningitis-negative individuals. Pathway analysis indicated that perturbed energy metabolism might be the cause of a number of metabolic changes in the CSF of patients with TBM. Differences in brain metabolism in patients with TBM mainly involved carbohydrate and amino acid metabolism, consistent with previous studies. Further larger-scale research involving multiple institutions, more patients, and more types of meningitis at different disease stages will be needed to evaluate the diagnostic value of the identified metabolites to account for heterogeneous genetic backgrounds, environmental factors, pathogens and measurement strategies.

Author contributions

All authors listed have made a substantial, direct and intellectual contribution to the work, and approved it for publication.

Conflict of interest statement

The authors declare that the research was conducted in the absence of any commercial or financial relationships that could be construed as a potential conflict of interest.

Acknowledgments

The study was supported by the Surface Project (81671186) from the National Natural Science Foundation of China.

Appendix A. Supplementary data

Supplementary data to this article can be found online at https://doi.org/10.1016/j.meegid.2019.01.003.

References

Ady Enche, C.N.A., Lim, S.M., Teh, L.K., Sallen, M.Z., Chin, A.V., Tan, M.P., Poi, P.J.H., Kamaruzzaman, S.B., Abdul Majeed, A.B., Ramasamy, K., 2017. Metabolomic-guided discovery of Alzheimer's disease biomarkers from body fluid. J. Neurosci. Res. 95, 2005–2024.

Andersen, A.D., Binzer, M., Stenager, E., Gramsbergen, J.B., 2017. Cerebrospinal fluid biomarkers for Parkinson's disease-a systematic review. Acta Neurol. Scand. 135, 34–56.

Bahr, N.C., Boulware, D.R., 2014. Methods of rapid diagnosis for the etiology of meningitis in adults. Biomark. Med 8, 1085–1103.

Bang, N.D., Caws, M., Truc, T.T., Duong, T.N., Dung, N.H., Ha, D.T., Thwaites, G.E., Heemskerk, D., Tarning, J., Merson, L., van Toi, P., Farrar, J.J., Wolbers, M., Pouplin, T., Day, J.N., 2016. Clinical presentations, diagnosis, mortality and prognostic markers of tuberculous meningitis in Vietnamese children: a prospective descriptive study. BMC Infect. Dis. 16 (573).

Bhargava, P., Calabresi, P.A., 2016. Metabolomics in multiple sclerosis. Mult. Scler. 22, 451–460.

Boehme, C.C., Saacks, S., O'Brien, R.J., 2013. The changing landscape of diagnostic services for tuberculosis. Semin. Respir. Crit. Care. Med. 34, 17–31.

Boyles, T.H., Thwaites, G.E., 2015. Appropriate use of the Xpert MTB/RIF assay in suspected tuberculous meningitis. Int. J. Tuberc. Lung Dis. 19, 276–277.

Chatterji, T., Singh, S., Sen, M., Singh, A.K., Maurya, P.K., Husain, N., Srivastava, J.K., Mandal, S.K., Roy, R., 2016. Comprehensive 1H NMR metabolic profiling of body fluids for differentiation of meningitis in adults. Metabolomics 12 (130).

Chen, P., Shi, M., Feng, G.D., Liu, J.Y., Wang, B.J., Shi, X.D., Ma, L., Liu, X.D., Yang, Y.N., Dai, W., Liu, T.T., He, Y., Li, J.G., Hao, X.K., Zhao, G., 2012a. A highly efficient Ziehl-Neelsen stain: identifying de novo intracellular Mycobacterium tuberculosis and improving detection of extracellular M. tuberculosis in cerebrospinal fluid. J. Clin. Microbiol. 50, 1166–1170.

Chen, Z., Wang, Y., Zeng, A., Chen, L., Wu, R., Chen, B., Chen, M., Bo, J., Zhang, H., Peng, Q., Lu, J., Meng, Q.H., 2012b. The clinical diagnostic significance of cerebrospinal fluid D-lactate for bacterial meningitis. Clin. Chim. Acta 413, 1512–1515.

Chiang, S.S., Khan, F.A., Milstein, M.B., Tolman, A.W., Benedetti, A., Starke, J.R., Becerra, M.C., 2014. Treatment outcomes of childhood tuberculous meningitis: a systematic review and meta-analysis. Lancet Infect. Dis. 14, 947–957.

Corston, R.N., McGale, E.H., Stonier, C., Hutchinson, E.C., Aber, G.M., 1981. Cerebrospinal fluid amino acid concentrations in patients with viral and tuberculous meningitis. J. Neurol. Neurosurg. Psychiatry 44, 791–795.

Croze, M.L., Soulage, C.O., 2013. Potential role and therapeutic interests of myo-inositol in metabolic diseases. Biochimie 95, 1811–1827.

Dai, Y.N., Huang, H.J., Song, W.Y., Tong, Y.X., Yang, D.H., Wang, M.S., Huang, Y.C., Chen, M.J., Zhang, J.J., Ren, Z.Z., Zheng, W., Pan, H.Y., 2017. Identification of potential metabolic biomarkers of cerebrospinal fluids that differentiate tuberculous meningitis from other types of meningitis by a metabolomics study. Oncotarget 8, 100095–100112.

Denkinger, C.M., Schumacher, S.G., Boehme, C.C., Dendukuri, N., Pai, M., Steingart, K.R., 2014. Xpert MTB/RIF assay for the diagnosis of extrapulmonary tuberculosis: a systematic review and meta-analysis. Eur. Respir. J. 44, 435–446.

Doern, C.D., Butler-Wu, S.M., 2016. Emerging and future applications of matrix-assisted laser desorption ionization time-of-flight (MALDI-TOF) mass spectrometry in the clinical microbiology laboratory: A Report of the Association for Molecular Pathology. J. Mol. Diagn. 18, 789–802.

Donald, P.R., Malan, C., 1985. Cerebrospinal fluid lactate and lactate dehydrogenase levels as diagnostic aids in tuberculous meningitis. S. Afr. Med. J. 67, 19–20.

Fennely, K.P., Morais, C.G., Hadad, D.J., Vinhas, S., Dietze, R., Palaci, M., 2012. The small membrane filter method of microscopy to diagnose pulmonary tuberculosis. J. Clin. Microbiol. 50, 2096–2099.

Giulieri, S., Chapuis-Taillard, C., Jaton, K., Cometta, A., Chuard, C., Hugli, O., du Pasquier, R., Bille, J., Meylan, P., Manuel, O., Marchetti, O., 2015. CSF lactate for accurate diagnosis of community-acquired bacterial meningitis. Eur. J. Clin. Microbiol. Infect. Dis. 34, 2049–2055.

Gomes, T., Reis-Santos, B., Bertolde, A., Johnson, J.L., Riley, L.W., Maciel, E.L., 2014. Epidemiology of extrapulmonary tuberculosis in Brazil: a hierarchical model. BMC Infect. Dis. 14 (9).

Graham, S.M., Donald, P.R., 2014. Death and disability: the outcomes of tuberculous meningitis. Lancet Infect. Dis. 14, 902–904.

Hristea, A., Olaru, I.D., Baicus, C., Moroti, R., Arama, V., Ion, M., 2012. Clinical prediction rule for differentiating tuberculous from viral meningitis. Int. J. Tuberc. Lung Dis. 16, 793–798.

Lawn, S.D., Kerkhoff, A.D., Burton, R., Schutz, C., Boulle, A., Vogt, M., Gupta-Wright, A., Nicol, M.P., Meintjes, G., 2017. Diagnostic accuracy, incremental yield and prognostic value of Determine TB-LAM for routine diagnostic testing for tuberculosis in HIV-infected patients requiring acute hospital admission in South Africa: a prospective cohort. BMC Med. 15 (67).

Lekhak, S.P., Sharma, L., Rajbhandari, R., Rajbhandari, P., Shrestha, R., Pant, B., 2016. Evaluation of multiplex PCR using MPB64 and IS6110 primers for rapid diagnosis of tuberculous meningitis. Tuberculosis (Edinb). 100, 1–4.

Li, Z.H., Du, B.P., Li, J., Zhang, J.L., Zheng, X.J., Jia, H.Y., Xing, A.Y., Sun, Q., Liu, F., Zhang, Z.D., 2017. Cerebrospinal fluid metabolomic profiling in tuberculous and viral meningitis: Screening potential markers for differential diagnosis. Clin. Chim. Acta 466, 38–45.

Ling, Y.S., Liang, H.J., Chung, M.H., Lin, M.H., Lin, C.Y., 2014. NMR- and MS-based metabolomics: various organ responses following naphthalene intervention. Mol. BioSyst. 10, 1918–1931.

Mai, N.T., Thwaites, G.E., 2017. Recent advances in the diagnosis and management of tuberculous meningitis. Curr. Opin. Infect. Dis. 30, 123–128.

Marais, S., Thwaites, G.E., Schoeman, J.F., Török, M.E., Misra, U.K., Prasad, K., Donald, P.R., Wilkinson, R.J., Marais, B.J., 2010. Tuberculous meningitis: a uniform case definition for use in clinical research. Lancet Infect. Dis. 10, 803–812.

Mason, S., van Furth, A.M.T., Mienie, L.J., Engelke, U.F., Wevers, R.A., Solomons, R., Reinecke, C.J., 2015. A hypothetical astrocyte-microglia lactate shuttle derived from a 1H NMR metabolomics analysis of cerebrospinal fluid from a cohort of South African children with tuberculous meningitis. Metabolomics 11, 822–837.

Mason, S., Reinecke, C.J., Kulik, W., van Cruchten, A., Solomons, R., van Furth, A.M., 2016a. Cerebrospinal fluid in tuberculous meningitis exhibits only the L-enantiomer of lactic acid. BMC Infect. Dis. 16 (251).

Mason, S., van Furth, A.M.T., Solomons, R., Wevers, R.A., van Reenen, M., Reinecke, C.J., 2016b. A putative urinary biosignature for diagnosis and follow-up of tuberculous meningitis in children: outcome of a metabolomics study disclosing host-pathogen responses. Metabolomics 12, 110.

Mason, S., Reinecke, C.J., Solomons, R., 2017. Cerebrospinal fluid amino acid profiling of pediatric cases with tuberculous meningitis. Front. Neurosci. 11 (534).

Molicotti, P., Bua, A., Zanetti, S., 2014. Cost-effectiveness in the diagnosis of tuberculosis: choices in developing countries. J. Infect. Dev. Ctries. 8, 24–38.

Patti, G.J., Yanes, O., Siuzdak, G., 2012. Innovation: metabolomics: the apogee of the omics trilogy. Nat. Rev. Mol. Cell Biol. 13, 263–269.

Pormohammad, A., Riahi, S.M., Nasiri, M.J., Fallah, F., Aghazadeh, M., Doustdar, F., Pouriran, R., 2017. Diagnostic test accuracy of adenosine deaminase for tuberculous meningitis: a systematic review and meta-analysis. J. Inf. Secur. 74, 545–554.

Qureshi, G.A., Baig, S.M., Bednar, I., Halawa, A., Parvez, S.H., 1998. The neurochemical markers in cerebrospinal fluid to differentiate between aseptic and tuberculous meningitis. Neurochem. Int. 32, 197–203.

Rodríguez-Núñez, A., Camiña, F., Lojo, S., Rodríguez-Segade, S., Castro-Gago, M., 1993. Concentrations of nucleotides, nucleosides, purine bases and urate in cerebrospinal fluid of children with meningitis. Acta Paediatr. 82, 849–852.

Rufai, S.B., Singh, A., Singh, J., Kumar, P., Sankar, M.M., Singh, S., 2017. Diagnostic usefulness of Xpert MTB/RIF assay for detection of tuberculous meningitis using cerebrospinal fluid. J. Inf. Secur. 75, 125–131.

Sanaei Dashti, A., Alizadeh, S., Karimi, A., Khalifeh, M., Shoja, S.A., 2017. Diagnostic value of lactate, procalcitonin, ferritin, serum-C-reactive protein, and other biomarkers in bacterial and viral meningitis: a cross-sectional study. Medicine (Baltimore) 96, e7637.
Shim, J., Shin, Y., Lee, I., Kim, S.Y., 2017. L-methionine production. Adv. Biochem. Eng. Biotechnol. 159, 153–177.
Sperringer, J.E., Addington, A., Hutson, S.M., 2017. Branched-chain amino acids and brain metabolism. Neurochem. Res. 42, 1697–1709.
Thapar, R., Titus, M.A., 2014. Recent advances in metabolic profiling and imaging of prostate cancer. Curr. Metabolomics 2, 53–69.
Thwaites, G.E., Simmons, C.P., Than Ha Quyen, N., Thi Hong Chau, T., Phuong Mai, P., Thi Dung, N., Hoan Phu, N., White, N.P., Tinh Hien, T., Farrar, J.J., 2003. Pathophysiology and prognosis in Vietnamese adults with tuberculous meningitis. J. Infect. Dis. 188, 1105–1115.
Török, M.E., 2015. Tuberculous meningitis: advances in diagnosis and treatment. Br. Med. Bull. 113, 117–131.
Tunkel, A.R., Hartman, B.J., Kaplan, S.L., Kaufman, B.A., Roos, K.L., Scheld, W.M., Whitley, R.J., 2004. Practice guidelines for the management of bacterial meningitis. Clin. Infect. Dis. 39, 1267–1284.
Wei, Y., Wan, C.L., Xue, R., Li, X.J., Zhang, W.J., Pei, F.K., 2016. 1H NMR-based metabolomics study on urine form Haematitum-treated rats. Chin. J. Anal. Chem. 44, 857–963.
Wilkinson, R.J., Rohlwink, U., Misra, U.K., van Crevel, R., Mai, N.T.H., Dooley, K.E., Caws, M., Figaji, A., Savic, R., Solomons, R., Thwaites, G.E., 2017. Tuberculous meningitis. Nat. Rev. Neurol. 13, 581–598.
Xia, J., Wishart, D.S., 2010. MSEA: a web-based tool to identify biologically meaningful patterns in quantitative metabolomic data. Nucleic Acids Res. 38, W71–W77.
Xia, J., Sinelnikov, I.V., Han, B., Wishart, D.S., 2015. MetaboAnalyst 3.0-making metabolomics more meaningful. Nucleic Acids Res. 43, W251–W257.
Yu, J., Wang, Z.J., Chen, L.H., Li, H.H., 2016. Diagnostic accuracy of interferon-gamma release assays for tuberculous meningitis: a meta-analysis. Int. J. Tuberc. Lung. Dis. 20, 494–499.
Zampieri, M., Sekar, K., Zamboni, N., Sauer, U., 2017. Frontiers of high-throughput metabolomics. Curr. Opin. Chem. Biol. 36, 15–23.